Biochemistry

pubs.acs.org/biochemistry Article

Phosphomimetic Mutation at Ser165 of α-Tubulin Promotes the Persistence of GTP Caps in Microtubules

Vinay Maddula, Nathalia S. Holtzman, Maria C. Nagan,*,# and Susan A. Rotenberg*,#

Cite This: *Biochemistry* 2022, 61, 1508−1516 Read Online

ACCESS | Metrics & More | Article Recommendations | Supporting Information

ABSTRACT: Protein kinase C (PKC)-mediated phosphorylation of α-tubulin at Ser165 or expression of phosphomimetic (S165D)-α-tubulin stimulates microtubule (MT) polymerization (*Cytoskeleton* **2014**, *71*, 257−272). Ser165 lies near the interface between adjacent αβ-tubulin heterodimers and helix H8, which contains Glu254, the catalytic residue in α-tubulin that hydrolyzes the exchangeable GTP in β-tubulin (β:GTP) and triggers MT depolymerization. It was hypothesized that S165D, a phosphomimetic variant of α-tubulin, perturbs the alignment of α:Glu254 with respect to β:GTP, thereby impairing its hydrolysis. Molecular simulations were performed with cryoEM structures of MTs (PDB ID: 3J6E) in which phosphomimetic S165D or control S165N had been substituted. Unlike native and S165N structures, the distance between S165D and α:Glu254 increased by 0.6 Å, while the distance between α:Glu254 and β:GTP decreased by 0.4 Å. Rotation of β:GTP by 4 Å occurred in the S165D variant, whereas β:GTP in the S165N control was unchanged from the native structure. Additionally, the S165D variant exhibited an altered pattern of H-bonding to β:GTP, including the loss of three H-bonds. The significance of these findings to β:GTP hydrolysis was analyzed in MCF-10A human breast cells treated with an antibody that detects GTP-bound tubulin. Compared with controls, GTP−tubulin signals were at higher levels in cells that ectopically expressed S165D-α-tubulin (TUBA1C) or had been treated with PKC activator DAG-lactone to induce phosphorylation of Ser165 in native α-tubulin. These findings support a model whereby conformational changes induced by Ser165 phosphorylation alter the spatial relationship between β:GTP and α:Glu254, thereby slowing GTP hydrolysis and promoting GTP caps.

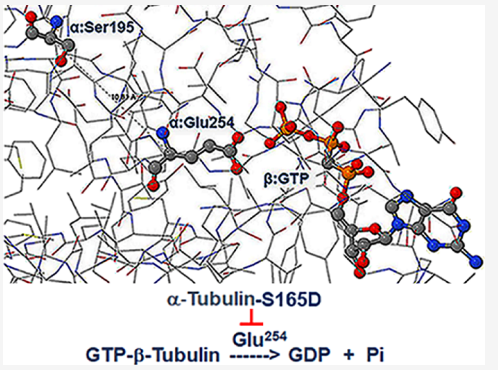

INTRODUCTION

Microtubules (MTs) are composed of an array of polymers consisting of heterodimeric protein αβ-tubulin.[1] As a fundamental element in the cytoskeleton, microtubules are known to be important in eukaryotic cell motility, cell division, and cellular transport functions.[2] The stochastic growth and shortening during polymerization of MTs, known as dynamic instability, is dependent on the hydrolysis of GTP bound at the exchangeable site (E-site) of β-tubulin.[3] Rapid microtubule dynamics are observed during mitosis,[4] and thus, a number of tubulin-binding agents have been developed as chemotherapy agents.[5,6]

Protein kinase Cα (PKCα) has been associated with particularly aggressive breast cancer tumors.[7] PKCα is known to phosphorylate Ser165 in α-tubulin and thereby increase the motility of non-transformed MCF-10A human breast cells.[8] Substitution of Ser165 with a negatively charged Asp residue (S165D) that mimics phosphorylated Ser165 results in cell motility similar to that induced by diacylglycerol lactone (DAG), a membrane-permeable PKC activator.[9] In contrast, substitution of Ser165 with a neutral amino acid such as Asn (S165N) inhibits PKCα-induced motility. The impact by either DAG-stimulated Ser165 phosphorylation or expression of the S165D mutant on MT dynamics was demonstrated by an increased rate of MT growth and a prolonged growth phase.[10] However, expression of the S165N mutant had reciprocal effects on these parameters. In view of these and other findings,[11] phosphorylation of α-tubulin at Ser165 in α-tubulin is proposed to be a toggle switch that reciprocally controls cell motility and proliferation of human breast tumor cells.

Assembly of αβ-tubulin heterodimers into MTs occurs while there is a GTP bound at the E-site of each of several β-tubulin units (β:GTP) at the growing end, known as a "GTP cap". This GTP is bound at the longitudinal interface between α- and β-tubulin subunits of two adjacent heterodimers (the inter-dimer cleft) (Figure 1A). In the GTP-bound state, MTs are stabilized and undergo polymerization.[12−16] When β:GTP is hydrolyzed, MTs are destabilized and consequently disassemble through the process of catastrophe. Complete

Received: March 17, 2022
Revised: June 24, 2022
Published: July 8, 2022

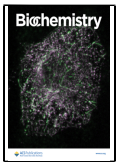

https://doi.org/10.1021/acs.biochem.2c00154
Biochemistry 2022, 61, 1508−1516

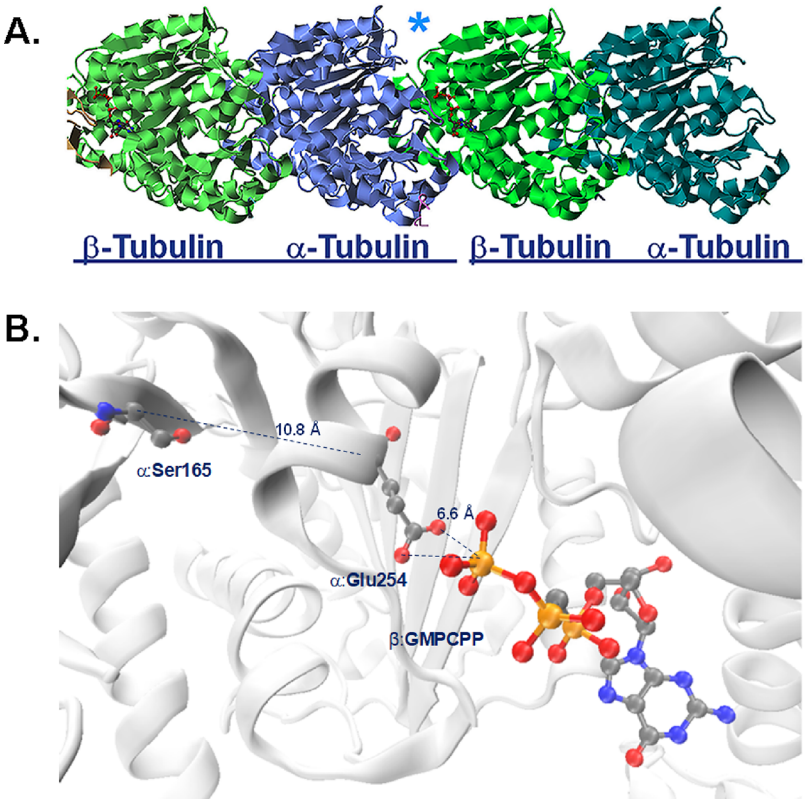

Figure 1. Model of the inter-dimer cleft in a native tubulin polymer. The interface between two $\alpha\beta$-tubulin heterodimers of a microtubule polymer (PDB ID: 3J6E) was viewed with AMBER software. (A) The inter-dimer cleft is marked by an asterisk (*). Visible within each β-subunit is a ball-and-stick structure (RGB colors) of the non-hydrolyzable GTP analogue GMPCPP. (B) Close proximity of α:Ser165 and α:Glu254 is depicted by the distance between their α-carbons (10.8 Å). Also shown is the distance between α-Glu254, starting from either carboxylate oxygen (red), and the γ-phosphorous atom (orange) of the guanine nucleotide (6.6 Å).

disassembly can be averted if they are rescued by the addition of a short run of GTP-bound β-tubulin subunits.[3] Thus, the rate of GTP hydrolysis contributes to the dynamic instability of MTs.

Hydrolysis of β:GTP to GDP is mediated exclusively by Glu254 in α-tubulin (α:Glu254), as was originally shown in a yeast model.[13,17] This catalytic residue lies within helix H8 (Asp251 − Val260) that lies near the inter-dimer cleft, approximately 5 Å away from its substrate, the γ-phosphate of β:GTP (Figure 1B). Residues in helix H8 and contiguous T7 loop in the α-subunit are involved in longitudinal contacts with the β-subunit of the adjacent heterodimer.[18,19] Ser165 in α-tubulin (α:Ser165) is positioned approximately 10 Å from α:Glu254. Prompted by a structural model of previous findings,[9] we hypothesized that phosphorylation at Ser165 in α-tubulin perturbs the alignment of Glu254 relative to the γ-phosphate of β:GTP thereby preventing its hydrolysis and consequently promoting polymerization of MTs.

In order to gain a deeper understanding of the molecular ramifications of Ser165 phosphorylation, we investigated whether the substitution of Ser165 with Asp(D) or control Asn (N) affects the spatial positions of helix H8, β:GTP, and other key residues at the inter-dimer cleft between $\alpha\beta$-tubulin heterodimers. High-resolution cryo-electron microscopy (cryo-EM) structures of microtubules with GTP or GDP bound to β-tubulin made possible a more detailed investigation into the structural adjustments that result from the modification of Ser165.[17,19,20] Adjacent $\alpha\beta$-tubulin heterodimers within these cryo-EM structures were simulated at the atomic level. Our findings revealed several changes induced by the expression of the S165D-α-tubulin that were not evident in either the native structure (with Ser165) or the control S165N-α-tubulin. Notable differences included the spatial position and H-bonding environment of β:GTP. These effects were shown experimentally to correlate with the appearance of detectable GTP caps. This work provides further insight into how the phosphorylation of α-tubulin at a single site can alter the structure and dynamic behavior of MTs.[9]

MATERIALS AND METHODS

Systems. Three systems of $\alpha\beta$-tubulin consisting of the native sequence Ser165 in α-tubulin or substitutions at Ser165, namely, S165D or S165N, were built from the cryo-EM structures of a native porcine kinesin-decorated, GMPCPP-stabilized MT (EMDB: 5895; PDB ID: 3J6E).[19] Chains A and P of the cryo-EM structure were used to model the interface between α- and β-subunits at the inter-dimer cleft. Consistent with the cryo-EM structure, both α- and β-subunits contained GTP and Mg^{2+}. The β-subunit E-site of the cryo-EM structure originally contained GMPCPP, a non-hydrolyzable GTP analogue. For this study, GMPCPP was changed to GTP by replacing C3A with O3A. The three variants used for analysis are referred to as Ser165•GTP, S165N•GTP, and S165D•GTP. Similarly, simulations containing β:GDP were also carried out for α:Ser165 and the α:S165D variant of $\alpha\beta$-tubulin beginning from PDB ID: 3J6F (EMDB: 5896) and are referred to as Ser165•GDP and S165D•GDP, respectively. Hydrogens were added with the LEaP module of AMBER.[21]

https://doi.org/10.1021/acs.biochem.2c00154
Biochemistry 2022, 61, 1508−1516

In all structures, a loop of 10 aa residues (residues 39−48) in the α-subunit was missing from the cryo-EM structure due to the inherent flexibility of loop regions. SWISS-MODEL[22] located an exact match to the missing loop in a dynein homologue (PDB ID: 3J1T).[23] To insert the missing loop in the protein, the distance between the loop ends and the rest of the protein were minimized iteratively with decreasing harmonic restraints in a generalized-Born implicit solvent environment with a dielectric continuum (ε = 78.3) and mbondi3 atomic radii.[24]

All proteins were solvated with at least 10 Å of TIP4PEW water[25] beyond the solute in a truncated octahedral box. The net charge of the system was neutralized with K^+ ions and additionally buffered with 200 mM KCl. The protein was modeled with the ff14SB force field.[26] Revised Carlson parameters for GTP,[26] Åqvist parameters for Mg^{2+},[27] and balanced K^+ and Cl^- Joung and Cheatham monovalent ion parameters[28,29] developed for TIP4PEW water were employed. Systems were about 400,000 atoms each.

Molecular Dynamics Simulations. Trajectories were propagated using SANDER for equilibration and the PMEMD GPU code of AMBER for production condition runs.[21] A constant pressure of 1 atm and temperature of 300 K were maintained throughout simulations with a Langevin thermostat. All systems were treated with periodic boundary conditions and particle-mesh Ewald treatment of electrostatics.[30] A standard equilibration protocol[31] was employed, and trajectories were propagated with a 2.0 fs time step with data collected every 1.0 ps. The system was run under production-run conditions for at least 120 ns for each system, and the last 100 ns were employed for statistics.

System Stability. Root-mean-square deviations (RMSDs) from starting and average structures of α- and β-tubulin subunits were calculated for each system (Figure S1, Supporting Information). RMSDs from starting and average structures were stable throughout the simulations.

Analysis. Distances between heavy atoms were calculated with the CPPTRAJ module of AMBER.[21] Hydrogen bonds were analyzed in the system over time. A hydrogen bond was considered present between heavy atoms if the distance measures ≤3.5 Å and a heavy atom−H−heavy atom angle of 180 ± 45° is observed.

Cell Culture and Immunocytochemistry. All biochemical reagents were purchased from Sigma-Aldrich (St. Louis, MO) except where noted. The GTP−tubulin antibody (MB11) was obtained from AdipoGen Life Sciences (San Diego, CA), the α-tubulin antibody (Epitomics EP13324) was purchased from Abcam (Waltham, MA), and the myc-tag antibody (clone 4A6) was purchased from Millipore Sigma (Burlington, MA). Secondary antibodies goat anti-rabbit Alexa-546 and goat anti-human Alexa-488 were purchased from Fisher Scientific (Boston, MA), and goat anti-mouse DyLight 405 was obtained from BioLegend (San Diego, CA). The DAG-lactone reagent (JH-131E-153), provided by Victor Marquez (NCI-Frederick), was described elsewhere.[32] Construction and validation of plasmids encoding human α6-tubulin proteins (TUBA1C) were described elsewhere.[9]

Sample preparation used for the different conditions were directly comparable. MCF-10A cells were grown in complete medium on 10 cm Falcon culture dishes as previously described.[8] To prepare for the experiment, cells were replated at low density on 35 mm polylysine-coated glass-bottom plates (P35G-1.5-14-C) (MatTek Corp, Ashland, MA). The following day, cells were treated with 10 μM diacylglycerol lactone (DAG-lactone) or DMSO (0.1% v/v) for 30 min at 37 °C followed by immunocytochemistry. For transfection of a myc-tagged α-tubulin mutant plasmid cDNA into MCF-10A cells, cells were plated at 50% confluence in a 24-well plate and, on the next day, transfected with 0.5 μg plasmid using Lipofectamine-3000 (Life Technologies) according to the manufacturer's instructions. After 48 h, transfected cells were recovered and replated at moderately low density on glass bottom plates for 18−24 h, followed by immunocytochemistry.

The procedure used for immunocytochemistry was adapted from a previously reported method.[33] Cells were washed 3× with PEM-G buffer (80 mM PIPES (pH 6.9), 1 mM EGTA (ethylene glycol-bis(β-aminoethyl ether)-*N*,*N*,*N*′,*N*′-tetraacetic acid), 1 mM $MgCl_2$, and 10% glycerol (v/v) warmed to 37 °C and permeabilized for 3 min at 37 °C in PEM-G buffer containing 0.5% TritonX-100 plus 1 μM paclitaxel. Cells were washed 2× with PEM-G containing 1 μM paclitaxel and incubated for 15 min at 37 °C with GTP−tubulin-specific MB11 antibody diluted 1:5000 in warm incubation buffer (PEM-G containing 0.2% bovine serum albumin (BSA) and 1 μM paclitaxel), followed by washing 3× with warm incubation buffer. A secondary antibody goat anti-human Alexa-488 (Fisher Scientific) that had been diluted 1:1000 in warm incubation buffer was added to cells for 15 min at 37 °C, followed by washing 3× with warm incubation buffer. Cells were fixed for 15 min at room temperature by adding 4% paraformaldehyde (pH 7.4) in PBS. After washing twice with PBS containing 0.05% Tween-20 (PBST), cells were incubated with block buffer (PBST with 0.02% BSA) for 1 h at room temperature in a humidified chamber, followed by two washes with PBST. Anti-α-tubulin rabbit monoclonal antibody EP1332Y diluted 1:500 in PBST was added to the fixed cells and incubated in a humidified chamber overnight at room temperature. For transfected cells, mouse monoclonal myc-tag antibody (clone 4A6; 1:500) was included with anti-α-tubulin for the overnight incubation.

The following day, cells were washed 3× with PBST, followed by treatment for 1 h in a humidified chamber with the appropriate secondary antibodies diluted 1:1000 in PBST. Secondary antibodies consisted of goat anti-rabbit Alexa-546 alone or combined with goat anti-mouse conjugated with DyLight 405 to detect myc-tagged α-tubulin in transfected cells. Cells were washed 3× with PBS and kept hydrated in PBS for microscopy performed on the same day. A minimum of three independent experiments were performed with cells treated with DAG-lactone (or DMSO) or transfected with plasmids encoding the α-tubulin mutants.

Confocal Microscopy and Image Analysis. All images were recorded using identical parameters. Cell images were collected using an inverted TCS-SP5 laser-scanning confocal microscope (Leica Microsystems) with either a 40× or 63× 1.4NA oil-immersion objective lens. Laser intensities were kept at 25−30%, and pinholes were typically set to 1 Airy unit.

Only samples with healthy cells plated at a moderate density were imaged. To ensure the validity of data analysis, all samples were prepared using the same method for immunocytochemistry. Each set of images was collected on the same day using identical confocal settings that had been used in all other trials. This was done by setting the histogram intensities of the control sample image (DMSO or VC) to those chosen for the control in the first of the series of trials. Only unmodified original images were used for quantification.

https://doi.org/10.1021/acs.biochem.2c00154
Biochemistry 2022, 61, 1508−1516

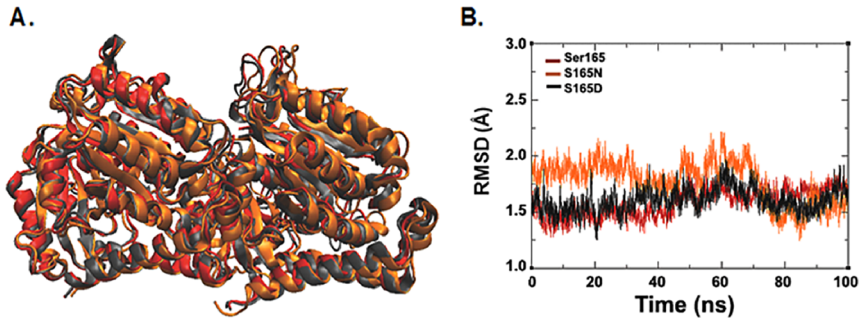

Figure 2. Global structures of $\alpha\beta$-tubulin. (A) Alignment of the β-subunits of $\alpha\beta$-tubulin with GTP bound. The native $\alpha\beta$-tubulin structure containing α:Ser165 is shown in red, the α:S165N variant is in orange, and the α:S165D variant is in dark gray. (B) Time-dependent plot of β-tubulin backbone-atom root-mean-square displacement (RMSD) over simulation time. Values are moving averages with windows over 10 ps. RMSD values are calculated relative to the $\alpha\beta$-tubulin starting structure of the native sequence and fitted to the α-tubulin subunit backbone. Full RMSD plots for α- and β-tubulin subunits are given in the Supporting Information (Figure S1).

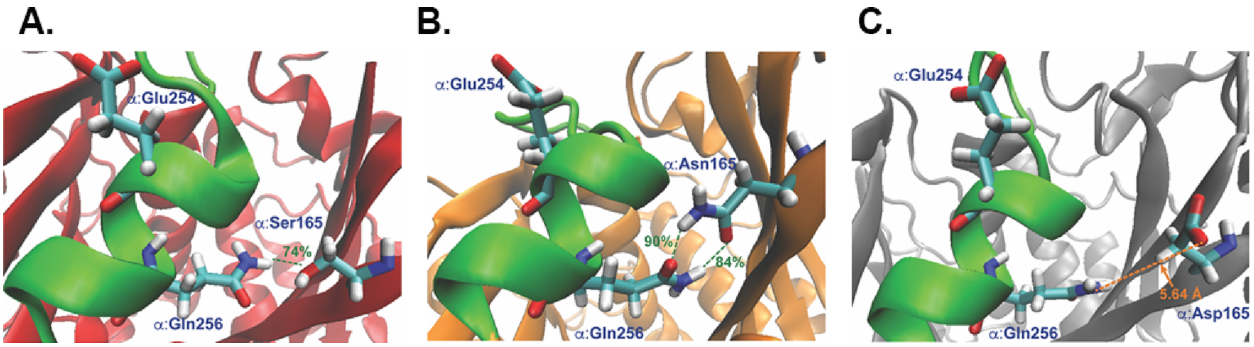

Figure 3. Interactions of residue-165 with Gln256 in neighboring α-helix H8. All residues reside in the α-subunit of $\alpha\beta$-tubulin. The catalytic α:Glu254 residue is shown as reference. The native Ser165 $\alpha\beta$-tubulin is red (A), S165N is orange (B), and S165D is gray (C). Hydrogen bonds and the percent of the simulation time that they were present are shown in green. Average distances are shown in orange.

Quantitative image analysis was performed in Photoshop on original images by determining the mean fluorescence intensities for green (G) and red (R) channels for each cell afforded by the histogram utility in Photoshop. Prior to measurement, the selection tool was used to encircle the cell in order to exclude error that would be introduced by the black background. An average G/R ratio (± SD) per cell was calculated for multiple cells in each condition. Statistical significance with images collected from at least three independent experiments was calculated by two-sample t test (DAG, DMSO) or one-way ANOVA (ectopic expression of α-tubulin proteins). To better illustrate the quantitative relationships determined from the original images, representative images for each type of experiment (e.g., ectopic expression of α-tubulin proteins) were enhanced as a block in Photoshop.

RESULTS AND DISCUSSION

Molecular Dynamics Measurements. For these modeling studies, we used a cryo-EM reconstruction of kinesin-decorated GMPCPP microtubules. The presence of kinesin is thought to aid in the alignment of α- and β-tubulin monomers[38] and therefore provided a more biologically relevant system. Adjacent $\alpha\beta$-heterodimers of a tubulin polymer (PDB ID: 3J6E) were visualized with Jmol software (version 14.32.25). In the native structure, the inter-dimer cleft (asterisk) along with the guanine nucleotide bound at the E-site in β-tubulin were evident (Figure 1A). A detailed view of the inter-dimer cleft (visualized with AMBER software) revealed the proximity of Ser165 to Glu254 in α-tubulin (α:Ser165, α:Glu254). As shown in Figure 1B, the Cα in Ser165 is 10.8 Å away from the Cα of Glu254 (Figure 1B). The distance between α:Glu254 and the γ-phosphorus of the guanine nucleotide (GMPCPP) in β-tubulin was observed to be 6.6 Å in the original cryoEM structure. For molecular dynamics simulations, the guanine nucleotide was modified to GTP.

Molecular dynamics simulations of three variants of $\alpha\beta$-tubulin (native Ser165•GTP, S165D•GTP, and S165N•GTP) were performed with GTP bound to the β-subunit in explicit water. Global structures of the three $\alpha\beta$-tubulin heterodimers were structurally similar over the course of the simulation time (Figure 2A). Alignment of backbone atoms in the β-subunits of all three $\alpha\beta$-tubulin GTP-bound structures resulted in similar backbone atom RMSD values relative to the starting structure of the native sequence (Figure 2B). Values were similar, relatively low (1.0−2.0 Å), and consistent throughout the simulation.

Differences were primarily local in nature when comparing the three GTP-bound $\alpha\beta$-tubulin structures, native Ser165•GTP, S165N•GTP, and S165D•GTP. As the site of phosphorylation in native α-tubulin, Ser165 was adjacent to helix H8 (Asp251−Val260), which included the catalytic residue Glu254 and nearby residue Gln256. Hydrogen bonding patterns around residue-165 in all three simulations revealed significant changes. In the native structure, a hydrogen bond between Ser165 and the Gln256 amino group was present for 74% of the simulation time (Figure 3A). Asn (N) substitution at aa165 was accommodated without perturbing the local structure. In the S165N variant, Gln256 rotated around the

https://doi.org/10.1021/acs.biochem.2c00154
Biochemistry 2022, 61, 1508−1516

CB-CG bond, repositioning the amide side chain to hydrogen bond with the Asn165 side chain (Figure 3B). In this complementary interaction, the Asn amino group hydrogen bonded with the carbonyl of Gln256 (90% of the simulation time) and the carbonyl group of Asn165 interacted with the Gln amino group (84%), effectively tightening the interaction between residue-165 and helix H8. In contrast, when Ser165 was substituted with Asp (D), the negatively charged carboxylate could not be accommodated by the crevice lying between itself and helix H8 (Figure 3C). The carboxylate group rotated 120° around the CA−CB bond, with the c1 angle[34,35] primarily t (98.8%, S165; 96.0%, S165N) to g^- (99.0%, S165D). This rotation in S165D reconfigured the carboxylate group toward the solvent and away from helix H8. As a result, the distance was increased between Asp165 OD1 and the Gln256 amino group nitrogen (5.6 ± 0.6 Å) and resulted in Asp165 hydrogen-bonding with Gln256 in only 2% of the simulation time. Thus, complementary hydrogen bond donors and acceptors in the S165N variant made substitution tolerable, and the residue 165-helix H8 interaction remained relatively unchanged.

In the S165D•GTP simulation, there was an increased distance between the residue-165 Cα position and residues of helix H8. Distances between the Cα positions of residue-165 and Gln256 or catalytic residue Glu254 increased in the S165D-α-tubulin variant by 1.1 and 0.6 Å, respectively, relative to the native Ser165 αβ-tubulin structure (Table 1). The

Table 1. Summary of Significant Atomic Distances around Helix H8, Res-165, and β:GTP[a]

αβ-tubulin system	distances (Å)		
	Res165:Cα-Gln256:Cα:	Res165:Cα-Glu254:Cα-	α:Glu254 OE1/2-β:GTP PG
Ser165•GTP	9.7 ± 0.3	10.8 ± 0.5	5.1 ± 0.3
S165N•GTP	9.9 ± 0.2	10.8 ± 0.3	5.2 ± 1.0
S165D•GTP	10.8 ± 0.3	11.4 ± 0.3	4.7 ± 0.7
Ser165•GDP	9.3 ± 0.6	10.1 ± 0.5	NA
S165D•GDP	9.7 ± 0.5	12.0 ± 0.6	NA

[a]Distances between C-alpha carbons (Cα) were measured between Res-165 and Gln256 or Glu254 within the α-tubulin subunit. The distance between the catalytic Glu254 is measured from an average of the two carboxylate oxygens (OE1 and OE2) and the γ-phosphorus of β:GTP (PG). NA, not applicable. Each distance represents the average (± SD) of 10^4 measurements.

displacement of helix H8 presumably resulted from electrostatic repulsions between the carboxylate groups of Asp165 and Glu254. This idea is supported by the absent or muted effects observed with the S165N variant where the distance to Glu254 was unchanged and the distance to Gln256 exhibited only a slight increase of 0.2 Å relative to the native structure. Similarly, in the GDP-bound system (Table 1), the distance between α:S165D and α:Glu254 (12.0 Å) was higher than that of native α:Ser165 (10.1 Å) and was more pronounced than the α:S165D/Glu254 distance in the GTP system (11.4 Å). The increased displacement of helix H8 away from S165D as compared with native Ser165 coincided with a shorter distance (4.7 Å vs 5.1 Å) between α:Glu254 and the hydrolyzable γ-phosphate of β:GTP (Table 1).

When structures were aligned on the native helix H8 backbone atoms (Figure 4), the N3 of the β:GTP base in the S165D structure was shifted by a distance of ∼4 Å and rotated by 10° (as measured by the angle between the vectors of α:Glu254:CA−β:GTP:N3).

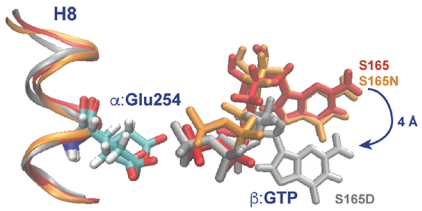

Figure 4. Impact of residue-165 variants on the position of β-tubulin GTP. Relative position of β-tubulin GTP in native Ser165 αβ-tubulin, red; S165N, orange; S165D, gray. Structures were aligned to the backbone atoms in helix H8 of the native Ser165 in α-tubulin using the first snapshot of the molecular dynamics trajectory. The catalytic residue Glu254 in α-tubulin is shown as a reference.

The interaction of residue-165 and helix H8 also perturbed the hydrogen bonding network between the α- and β-subunits at the inter-dimer cleft (Table 2). One particular hydrogen

Table 2. Hydrogen Bonding from within β-Tubulin to β:GTP in α:Ser165 Variants of αβ-Tubulin[a]

	Ser165	S165N	S165D
GTP O1A−β:Gln11 NH2	77%	70%	24%
β:Glu181 OE1/2−GTP 3′OH	71%	46%/33%	0%
β:Glu181 OE1/2−GTP 2′OH	46%	23%	0%
GTP O1B−β:Ser138 OH	91%	94%	0%
GTP O1B−β:Gly144 NH	6%	13%	64%

[a]A more complete list of H-bonding patterns of all three systems can be found in Table S1 and Figure S2 in the Supporting Information.

bond between the α-phosphate oxygen of GTP (αO1P−GTP) and the sidechain amino group of Gln11 in the β-subunit (β:Gln11) was present during the majority of the simulation (77%; Figure 5A) in the native Ser165•GTP structure with an α-phosphate to β:Gln11 distance of 2.9 Å on average. This interaction was also present in S165N•GTP αβ-tubulin (70%, average distance 3.3 Å; Figure 5B). However, in the S165D•GTP structure, the distance between the α-phosphate oxygen of GTP and the β:Gln11 amino group nitrogen markedly increased to 5.6 Å, thereby eliminating any interactions with GTP. Interestingly, a new hydrogen bond was identified in the S165D•GTP structure between α:Ala247 and β:Gln11 that was not present in the other two systems (Figure 5C; 42% of the simulation time). Ala247 in α-tubulin lies within loop T7, a highly conserved sequence that is contiguous with helix H8 and known to interact with GTP bound to β-tubulin in the adjacent heterodimer.[20] In S165D•GTP, while the hydrogen bond is not always present, this distance was on average 3.6 Å, far shorter than the distances in either native Ser165•GTP or S165N•GTP (6.0 and 6.7 Å, respectively). Both α:Ala247 and β:Gln11 were in close proximity to the β:GTP, making possible a new stabilizing interaction at the inter-dimer cleft.

Our evaluation of GDP-bound systems was limited to a comparison of the native Ser165•GDP and S165D•GDP. Some aspects of the S165D•GDP were unchanged from the native structure. For instance, in the GTP-containing S165D system, the α:Ala247 backbone oxygen and β:Gln11 amino group were only 3.6 Å apart (Figure 5C), but the distances in both Ser165•GDP and S165D•GDP (6.4 Å and 5.9 Å,

https://doi.org/10.1021/acs.biochem.2c00154
Biochemistry 2022, 61, 1508−1516

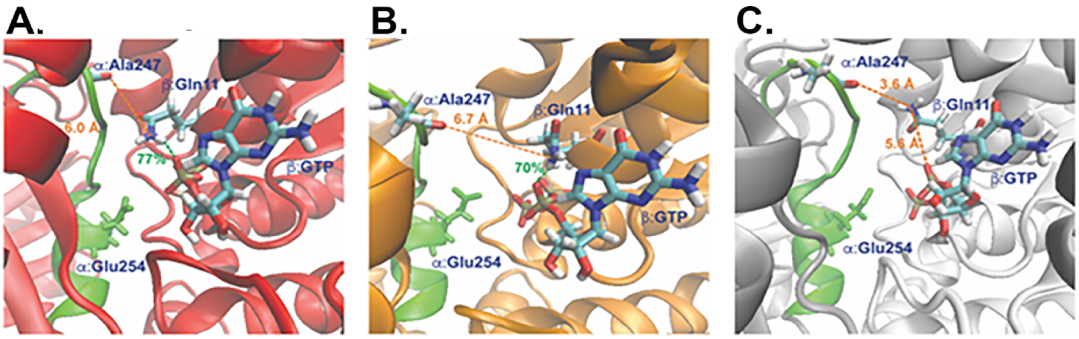

Figure 5. Impact of residue-165 on the hydrogen bonding pattern at the inter-dimer cleft. This view is a rotation 180° toward the viewer, across the horizontal axis from Figure 3. The alpha H8 helix (green) is shown for reference. Native Ser165 $\alpha\beta$-tubulin is red (A), S165N is orange (B), and S165D is gray (C). Hydrogen bonds and the percent of the simulation time present are shown in green. Average distances are shown in orange.

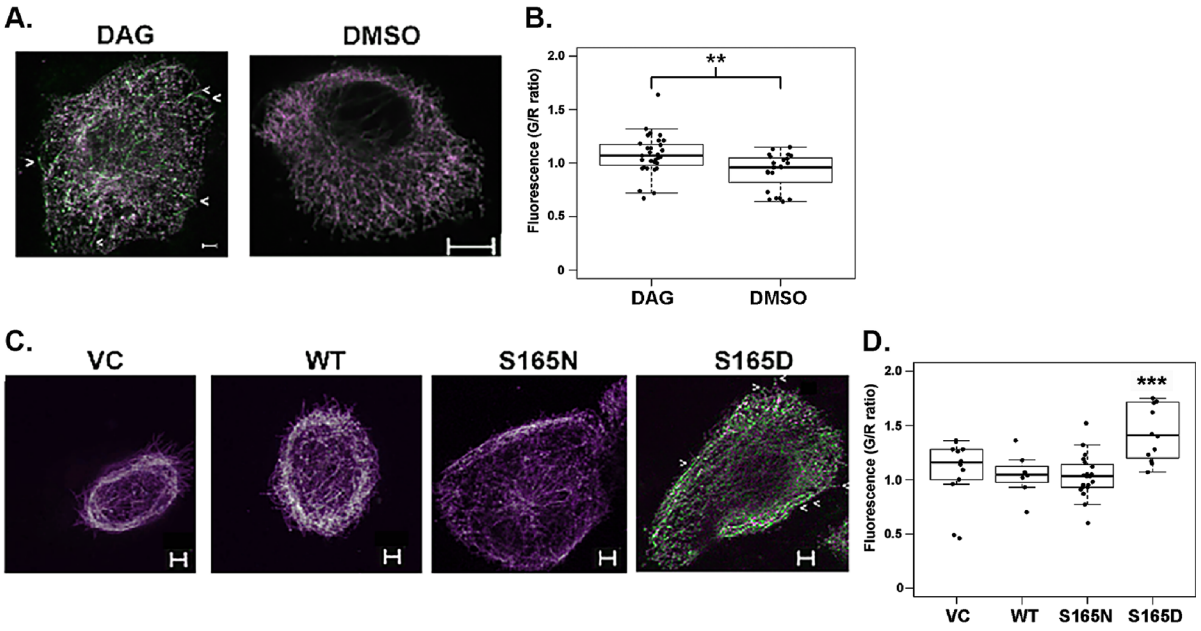

Figure 6. Detection of GTP-bound tubulin in MCF-10A cells after treatment with DAG-lactone or expression of mutant α-tubulin proteins. Cells were either (A) treated with 10 μM DAG-lactone (DAG) or DMSO (0.1% v/v) or (C) transfected with a plasmid encoding wildtype (WT), mutant α-tubulin (S165D or S165N), or the empty vector (VC). Cells were stained with human MB11 antibody to detect GTP caps (green) and counterstained with α-tubulin antibody (magenta) to detect MTs. Scale bar = 5 μm. (B, D) Cell images were quantified using the Photoshop histogram utility to record the mean fluorescence intensity in the green (G) and red (R) channels, followed by calculating the average G/R ratio (± SD) for each condition. Original unmodified images were analyzed from three independent experiments with ±DAG or ectopic expression of α-tubulin proteins. Total cell numbers inspected per condition were DAG, n = 30; DMSO, n = 23; S165D, n = 12; S165N, n = 20; WT, n = 8; and VC, n = 13. Quantification for (A) and (C) is shown in (B) and (D), respectively. Box plots show the raw data (dots), median (bold horizontal line), 25th and 75th percentiles (boxes), and outlier limits (upper and lower whiskers). (B) Statistical significance of differences in the G/R ratio was calculated by two-sample t test, $^{**}P < 0.01$. (D) The median G/R ratio for S165D was significantly greater than that for VC, WT, and S165N. Statistical significance was determined by one-way ANOVA, $^{***}P < 0.001$.

respectively) were more like that of the native Ser165•GTP structure (6.0 Å) (Figure 5A). However, the standard deviations in these distances in the GDP simulations were larger than those observed in the GTP-containing simulations (1.3 and 1.5 versus 0.6 and 0.8), indicating that the GDP-containing structures may be slightly more flexible at the interface. Upon further examination, several differences in the H-bonding pattern surrounding GDP were found. In this regard, the S165D•GDP system exhibited a loss of several H-bonds to GDP that were present in Ser165•GDP as well as all three GTP-bound systems. For additional details of these GDP-bound systems, see Table S2 in the Supporting Information.

In the GTP-bound systems, Table 2 documents some additional hydrogen bonds that were changed by S165D. (Further details are given in Table S1 and Figure S2 in the Supporting Information.) In addition to the loss of a hydrogen bond between β-Gln11 and the α-phosphate of GTP, other hydrogen bonds to GTP present in native Ser165•GTP and S165N•GTP for most of the simulation time were significantly decreased or lost in S165D•GTP (Table 2 and green lines in Figure 5). In the native Ser165•GTP and S165N•GTP variants, the β:Ser138 hydroxyl group was strongly bound to the GTP β-phosphate oxygen, exhibiting hydrogen bonding at 91 and 95% of the simulation time, respectively, but was completely lost in the S165D•GTP variant. (The loss of this hydrogen bond was also noted in the S165D•GDP system.)

https://doi.org/10.1021/acs.biochem.2c00154
Biochemistry 2022, 61, 1508−1516

Additionally, in the native Ser165 structure, β:Glu181 hydrogen bonded to both the 3′OH and 2′OH of the ribose moiety of β:GTP for 71 and 46% of the simulation time, respectively. During the simulation time, the S165N•GTP variant stabilized these sugar hydroxyls less often than in the native system, but the interactions were still present (46%-3′OH and 23%-2′OH). However, in the S165D•GTP system, β:Gln11, β:Ser138, and β:Glu181 were lost entirely as H-bonding partners. It is notable that these three residues are highly conserved in all 10 β-tubulin isotypes.[36] Taken together, the displacement of helix H8 coincident with rotation of the β:GTP base and remodeling of the H-bonding pattern to GTP all have potential implications for how well the guanine nucleotide can be positioned and consequently hydrolyzed. Whether or not these structural perturbations have significance for GTP hydrolysis will be addressed experimentally.

Detection of GTP Caps in Human Breast Cells. Our hypothesis is that the phosphomimetic mutant S165D and, analogously, the phosphorylation of Ser165 in α-tubulin leads to the structural misalignment of Glu254 relative to β:GTP. Consequently, if GTP hydrolysis is impaired, it would result in the retention of GTP caps at the growing ends of microtubules. In previous studies, we showed that diacylglycerol lactone (DAG), a membrane-permeable PKC activator, induced the phosphorylation of Ser165 in endogenous α-tubulin of MCF-10A human breast cells. Furthermore, this event altered the parameters of microtubule dynamics in a manner that could be reproduced in cells expressing S165D-α-tubulin.[9,10] Therefore, we investigated a role for α:Ser165 in controlling the level of observable GTP caps by treating cells with DAG or by overexpression of the wildtype α-tubulin (WT) or each mutant protein (S165D or S165N).

MTs in MCF-10A cells were analyzed for GTP caps by immunocytochemistry with the MB11 antibody, a conformation-sensitive probe that recognizes tubulin-bound GTP as either punctate signals along growing MTs or as short segments within an MT (islands). Since this antibody must be applied to detergent-permeabilized cells in the absence of a fixative, all buffers were supplemented with 1 μM paclitaxel as previously recommended.[33] This additive greatly improved the image clarity by stabilizing MTs and preserving their GTP-bound state. Sample preparation was performed identically with cells that had been (1) treated with DAG or DMSO or (2) transfected with a plasmid encoding the wildtype (WT) α-tubulin (TUBA1C), S165D- or S165N-α-tubulin mutant, or the empty vector (vector control, VC; see the Materials and Methods section).

The incidence of punctate signals corresponding to GTP caps was evaluated in MTs of MCF-10A cells treated with DAG to induce the PKC-mediated reversible phosphorylation of native α-tubulin at Ser165.[9] Compared with the vehicle control (DMSO), DAG-treated MCF-10A cells were characteristically larger, flatter, and dissociated from one another, thereby recapitulating the observed effects previously attributed to PKCα overexpression.[8] MTs were stained with the MB11 antibody to detect GTP-bound tubulin (green) and an α-tubulin-specific rabbit monoclonal antibody to counterstain total α-tubulin (magenta). Bright green punctate signals indicative of GTP caps were randomly distributed along the length of MTs in DAG-treated cells (Figure 6A). Although less frequent, green signals at the ends of a few microtubules (magenta) could be discerned at the cell periphery (indicated by a caret (<) in Figure 6A). GTP islands, thought to be the result of rescue events,[33,37] were prominent as short green segments that may have represented the accumulation of many GTP caps within a short distance. The high density of puncta at the cell edge was mostly associated with the cell surface in contact with the glass slide. In contrast, vehicle-treated cells had no detectable green punctate signals. The strong signals observed with DAG-lactone are presumed to be the result of slowed hydrolysis of β:GTP which would allow for the accumulation of GTP caps.

In a related experiment, we tested cells that ectopically expressed myc-tagged α-tubulin proteins that included the WT-, S165D-, and S165N-α-tubulin. Expression of each myc-tagged α-tubulin was verified by the presence of the myc signal (Figure S3, Supporting Information). With the S165D-α-tubulin mutant, a vivid pattern of green punctate signals was evident at the membrane surface (Figure 6C). Like DAG-treated cells, punctate signals in cells expressing the phosphomimetic mutant could be discerned along the length of MTs and at MT ends (carets) and were clustered at the cell surface in contact with the glass slide. In cells expressing the S165N mutant, signals were typically undetectable as shown in Figure 6C. In general, cells expressing either the WT-α-tubulin or empty vector (VC) displayed no detectable punctate signals (Figure 6C). The absence of punctate signals following overexpression of the WT protein argues against a dosage effect as the source of the signal.

Analysis of individual cells in original unmodified images was performed by determining the ratio of mean fluorescence intensities in the green (G) and red (R) channels. As shown in Figure 6B, DAG-treated cells produced a G/R ratio ± SD (1.08 ± 0.19) that was higher than vehicle-treated cells (0.92 ± 0.17) and was statistically significant ($P < 0.01$). In Figure 6D, cells expressing the S165D-α-tubulin mutant exhibited a substantially higher G/R ratio (1.44 ± 0.26) as compared with the S165N mutant (1.03 ± 0.2), WT α-tubulin (1.045 ± 0.19), and VC (1.08 ± 0.29) and proved to be statistically significant ($P < 0.001$). It is noted that the less robust effect measured for DAG-treated cells relative to the S165D mutant may have been the result of reversible phosphorylation, which cannot occur with a phosphomimetic mutant.

CONCLUSIONS

In this study, molecular simulations and experimental testing produced a model for how the phosphorylation of Ser165 in α-tubulin or its phosphomimetic analogue S165D stabilizes the GTP-bound state of tubulin polymers. The higher incidence of GTP−tubulin signals is consistent with the prolonged phase of MT polymerization that was previously ascribed to both forms.[10] Molecular dynamics showed that the S165D variant engendered a distinctly different chemical environment within the α-tubulin subunit at the inter-dimer cleft of a tubulin polymer. When compared with native Ser165 and S165N structures, strong perturbations were observed in the distance between the S165D residue and residues in helix H8 of α-tubulin, and in the H-bonding pattern around β:GTP at the inter-dimer interface. These seemingly small local changes coincided with rotation of the guanine base position and a loss of hydrogen bonding to β:GTP. Taken together, these findings support a model in which the phosphorylation of Ser165 slows the hydrolysis of the E-site GTP by altering the precise spatial relationship between α:Glu254 and the γ-phosphate of β:GTP. The differential signal patterns obtained experimentally with the GTP−tubulin antibody supported this prediction.

https://doi.org/10.1021/acs.biochem.2c00154
Biochemistry 2022, 61, 1508−1516

The use of molecular dynamics offered an elegant approach by which to identify specific structural features of $\alpha\beta$-tubulin that respond to phosphorylation at Ser165 in α-tubulin. The presented evidence that GTP hydrolysis is slowed by phosphorylation (DAG treatment) or by a phosphomimetic at Ser165 underscores the functional significance of these structural perturbations. In view of the critical importance of GTP hydrolysis to the MT structure and dynamic instability, molecular dynamics of the E-site GTP could be used as a predictive tool to evaluate the effects of other protein kinases on $\alpha\beta$-tubulin as well as for in *silico* screening of drugs for their potential to alter MT dynamic behavior.

■ ASSOCIATED CONTENT

Supporting Information

The Supporting Information is available free of charge at https://pubs.acs.org/doi/10.1021/acs.biochem.2c00154.

(Figure S1) RMSD of starting and average α- and β-subunit structures; (Figure S2) scheme depicting the hydrogen bonds between β-tubulin and β:GTP in α:Ser165 variants of $\alpha\beta$-tubulin; (Figure S3) expression of myc-tagged α-tubulin mutant proteins; (Table S1) list of hydrogen bonds between β-tubulin and β:GTP in α:Ser165 variants of $\alpha\beta$-tubulin (PDF)

Accession Codes

PDB ID: 3J6E (EMDB: 5895); PDB ID: 3J6F (EMDB: 5896).

■ AUTHOR INFORMATION

Corresponding Authors

Maria C. Nagan − *Department of Chemistry, Stony Brook University, Stony Brook, New York 11794-3400, United States*; Email: maria.nagan@stonybrook.edu

Susan A. Rotenberg − *Department of Chemistry & Biochemistry, Queens College − The City University of New York, Flushing, New York 11367-1597, United States; PhD Program in Biochemistry, The Graduate Center of The City University of New York, New York, New York 10016, United States*; orcid.org/0000-0002-6618-686X; Email: susan.rotenberg@qc.cuny.edu

Authors

Vinay Maddula − *Department of Chemistry, Adelphi University, Garden City, New York 11530, United States*

Nathalia S. Holtzman − *Department of Biology, Queens College − The City University of New York, Flushing, New York 11367-1597, United States; PhD Program in Biochemistry, The Graduate Center of The City University of New York, New York, New York 10016, United States*

Complete contact information is available at: https://pubs.acs.org/10.1021/acs.biochem.2c00154

Author Contributions

#M.C.N. and S.A.R. contributed equally to this work.

Author Contributions

The manuscript was written through contributions of all authors. All authors have given approval to the final version of the manuscript.

Funding

This work was funded by the National Science Foundation (CHE-0116435, CHE-0521063, CHE-0849677, and CHE-1229354) (to M.C.N.), the National Institutes of Health (CA125632) and PSC-CUNY (64051-00 52) (to S.A.R.).

Notes

The authors declare no competing financial interest.

■ ACKNOWLEDGMENTS

The authors thank Dr. Stephen S. Arnott (Queens College) for performing the statistical analysis, Prof. Radhika Subramanian (Harvard Medical School) for suggesting the MB11 antibody to detect GTP caps, and Dr. Victor Marquez (NCI-Frederick) for providing the DAG-lactone reagent (JH-131E-153). Confocal microscopy was performed in the Core Facility for Imaging, Cellular and Molecular Biology at Queens College.

■ ABBREVIATIONS

PKC, protein kinase C; MT, microtubule; DAG, diacylglycerol; GTP, guanosine triphosphate; GDP, guanosine diphosphate; GMPCPP, $\beta\gamma$-methyleneguanosine 5′-triphosphate; DMSO, dimethylsulfoxide

■ REFERENCES

(1) Luduena, R. F.; Woodward, D. O. Isolation and partial characterization of alpha and beta-tubulin from outer doublets of sea-urchin sperm and microtubules of chick-embryo brain. *Proc. Natl. Acad. Sci. U. S. A.* **1973**, *70*, 3594−3598.

(2) Hyams, J. S.; Lloyd, C. W. Microtubules. *Wiley-Liss: New York* **1994**.

(3) Mitchison, T.; Kirschner, M. Dynamic instability of microtubule growth. *Nature* **1984**, *312*, 237−242.

(4) Rusan, N. M.; Fagerstrom, C. J.; Yvon, A. M. C.; Wadsworth, P. Cell cycle-dependent changes in microtubule dynamics in living cells expressing green fluorescent protein-alpha tubulin. *Mol. Biol. Cell* **2001**, *12*, 971−980.

(5) Escriu, C.; Brenton, J. D. New Insights into Tubulin Binders. *In: Emerging Therapeutic Targets in Ovarian Cancer* 2011, pp. 259−278; Kaye, S., Brown, R., Gabra, H., Gore, M. (eds) Springer, New York, NY.

(6) Stanton, R. A.; Gernert, K. M.; Nettles, J. H.; Aneja, R. Drugs that target dynamic microtubules: A new molecular perspective. *Med. Res. Rev.* **2011**, *31*, 443−481.

(7) Lonne, G. K.; Cornmark, L.; Zahirovic, I. O.; Landberg, G.; Jirstrom, K.; Larsson, C. PKC alpha expression is a marker for breast cancer aggressiveness. *Mol. Cancer* **2010**, *9*, 76−90.

(8) Sun, X. G.; Rotenberg, S. A. Overexpression of protein kinase C alpha in MCF-10A human breast cells engenders dramatic alterations in morphology, proliferation, and motility. *Cell Growth Differ.* **1999**, *10*, 343−352.

(9) Abeyweera, T. P.; Chen, X. Y.; Rotenberg, S. A. Phosphorylation of α6-tubulin by protein kinase C alpha activates motility of human breast cells. *J. Biol. Chem.* **2009**, *284*, 17648−17656.

(10) De, S.; Tsimounis, A.; Chen, X. Y.; Rotenberg, S. A. Phosphorylation of alpha-tubulin by protein kinase C stimulates microtubule dynamics in human breast cells. *Cytoskeleton* **2014**, *71*, 257−272.

(11) Markovsky, E.; de Stanchina, E.; Itzkowitz, A.; Haimovitz-Friedman, A.; Rotenberg, S. A. Phosphorylation state of Ser165 in α-tubulin is a toggle switch that controls proliferating human breast tumors. *Cell Signal* **2018**, *52*, 74−82.

(12) Terry, B. J.; Purich, D. L. Assembly and disassembly properties of microtubules formed in the presence of GTP, 5′-guanylyl imidodiphosphate and 5′-guanylyl methylene diphosphate. *J. Biol. Chem.* **1980**, *255*, 532−536.

(13) Mejillano, M. R.; Barton, J. S.; Nath, J. P.; Himes, R. H. GTP analogs interact with the tubulin exchangeable site during assembly and upon binding. *Biochemistry* **1990**, *29*, 1208−1216.

(14) Seckler, R.; Wu, G. M.; Timasheff, S. N. Interactions of tubulin with guanylyl-(beta-gamma-methylene) diphosphonate - Formation and assembly of a stoichiometric complex. *J. Biol. Chem.* **1990**, *265*, 7655−7661.

(15) Hamel, E.; Lin, C. M. Reexamination of the role of nonhydrolyzable guanosine 5′-triphosphate analogs in tubulin polymerization - Reaction conditions are a critical factor for effective interactions at the exchangeable nucleotide site. *Biochemistry* **1990**, *29*, 2720−2729.
(16) Hyman, A. A.; Salser, S.; Drechsel, D. N.; Unwin, N.; Mitchison, T. J. Role of GTP hydrolysis in microtubule dynamics: information from a slowly hydrolyzable analogue. *GMPCPP. Mol. Biol. Cell* **1992**, *3*, 1155−1167.
(17) Richards, K. L.; Anders, K. R.; Nogales, E.; Schwartz, K.; Downing, K. H.; Botstein, D. Structure-function relationships in yeast tubulins. *Mol. Biol. Cell* **2000**, *11*, 1887−1903.
(18) Lowe, J.; Li, H.; Downing, K. H.; Nogales, E. Refined structure of alpha beta-tubulin at 3.5 A resolution. *J. Mol. Biol.* **2001**, *313*, 1045−1057.
(19) Alushin, G. M.; Lander, G. C.; Kellogg, E. H.; Zhang, R.; Baker, D.; Nogales, E. High-resolution microtubule structures reveal the structural transitions in alpha beta-tubulin upon GTP hydrolysis. *Cell* **2014**, *157*, 1117−1129.
(20) Nogales, E.; Wolf, S. G.; Downing, K. H. Structure of the alpha beta tubulin dimer by electron crystallography. *Nature* **1998**, *391*, 191−203.
(21) Case, D. A., *et al.*, *AMBER 2018*. University of California, San Francisco, 2018.
(22) Waterhouse, A.; Bertoni, M.; Bienert, S.; Studer, G.; Tauriello, G.; Gumienny, R.; Heer, F. T.; de Beer, T. A. P.; Rempfer, C.; Bordoli, L.; Lepore, R.; Schwede, T. SWISS-MODEL: homology modeling of protein structures and complexes. *Nucleic Acids Res.* **2018**, *46*, W296−W303.
(23) Redwine, W. B.; Hernandez-Lopez, R.; Zou, S. R.; Huang, J. L.; Reck-Peterson, S. L.; Leschziner, A. E. Structural basis for microtubule binding and release by dynein. *Science* **2012**, *337*, 1532−1536.
(24) Nguyen, H.; Roe, D. R.; Simmerling, C. Improved generalized born solvent model parameters for protein simulations. *J. Chem. Theory Comput.* **2013**, *9*, 2020−2034.
(25) Horn, H. W.; Swope Wc Fau, J. W.; Pitera Jw Fau - Madura, J. D.; Madura Jd Fau - Dick, T. J.; Dick Tj Fau, G. L.; Hura Gl Fau - Head-Gordon, T.; Head-Gordon, T. Development of an improved four-site water model for biomolecular simulations: TIP4P-Ew. *J. Chem. Phys.* **2004**, *120*, 9665−9678.
(26) Maier, J. A.; Martinez, C.; Kasavajhala, K.; Wickstrom, L.; Hauser, K. E.; Simmerling, C. ff14SB: Improving the accuracy of protein side chain and backbone parameters from ff99SB. *J. Chem. Theory Comput.* **2015**, *11*, 3696−3713.
(27) Meagher, K. L.; Redman, L. T.; Carlson, H. A. Development of polyphosphate parameters for use with the AMBER force field. *J. Comput. Chem.* **2003**, *24*, 1016−1025.
(28) Åqvist, J. Ion-water interaction potentials derived from free energy perturbation simulations. *J. Phys. Chem.* **1990**, *94*, 8021−8024.
(29) Joung, I. S.; Cheatham, T. E. Determination of alkali and halide monovalent ion parameters for use in explicitly solvated biomolecular simulations. *J. Phys. Chem. B* **2008**, *112*, 9020−9041.
(30) Darden, T.; York, D.; Pedersen, L. Particle mesh Ewald: An N·log(N) method for Ewald sums in large systems. *J. Chem. Phys.* **1993**, *98*, 10089−10092.
(31) Michael, L. A.; Chenault, J. A.; Miller, B. R., 3rd; Knolhoff, A. M.; Nagan, M. C. Water, shape recognition, salt bridges, and cation-pi interactions differentiate peptide recognition of the HIV rev-responsive element. *J. Mol. Biol.* **2009**, *392*, 774−786.
(32) Garcia-Bermejo, M. L.; Leskow, F. C.; Fuji, T.; Wang, Q.; Blumberg, P. M.; Ohba, M.; Kurok, T.; Han, K. C.; Lee, J.; Marquez, V. E.; Kazanietz, M. G. Diacylglycerol (DAG)-lactones, a new class of protein kinase C (PKC) agonists, induce apoptosis in LNCaP prostate cancer cells by selective activation of PKCalpha. *J. Biol. Chem.* **2002**, *277*, 645−655.
(33) deForges, H., Pilon, A., Pous, C., Perez, F. Imaging GTP-bound tubulin: From cellular to *in vitro* assembled microtubules. *In Methods in Cell Biology* 2013, *115*, 139−153. Elsevier, Inc.
(34) Dunbrack, R. L., Jr. Rotamer libraries in the 21st century. *Curr. Opin. Struct. Biol.* **2002**, *12*, 431−440.
(35) Lovell, S. C.; Word, J. M.; Richardson, J. S.; Richardson, D. C. The penultimate rotamer library. *Proteins* **2000**, *40*, 389−408.
(36) Huzil, J. T.; Chen, K.; Kurgan, L.; Tuszynski, J. A. The roles of *β*-tubulin mutations and isotype expression in acquired drug resistance. *Cancer Inf.* **2007**, *3*, 159−181.
(37) Dimitrov, A.; Quesnoit, M.; Moutel, S.; Cantaloube, I.; Pous, C.; Perez, F. Detection of GTP-tubulin conformation in vivo reveals a role for GTP remnants in microtubule rescues. *Science* **2008**, *322*, 1353−1356.

https://doi.org/10.1021/acs.biochem.2c00154
Biochemistry 2022, 61, 1508−1516